Atmos. Meas. Tech. Discuss., 3, 4865–4887, 2010
www.atmos-meas-tech-discuss.net/3/4865/2010/
doi:10.5194/amtd-3-4865-2010

Atmospheric Measurement Techniques Discussions

Camtracker: a new camera controlled high precision solar tracker system for FTIR-spectrometers

M. Gisi, F. Hase, S. Dohe, and T. Blumenstock

Karlsruhe Institute of Technology (KIT), Institute for Meteorology and Climate Research (IMK-ASF), Karlsruhe, Germany

Received: 29 October 2010 – Accepted: 2 November 2010 – Published: 9 November 2010

Correspondence to: M. Gisi (michael.gisi@kit.edu)

Published by Copernicus Publications on behalf of the European Geosciences Union.

Abstract

A new system to very precisely couple radiation of a moving source into a FTIR-spectrometer is presented. The Camtracker consists of a homemade altazimuthal solar tracker, a digital camera and a homemade program to process the camera data and to control the motion of the tracker. The key idea is to evaluate the image of the radiation source on the entrance field stop of the spectrometer. We prove that the system reaches tracking accuracies of about 10″ for a ground-based solar absorption FTIR spectrometer, which is significantly better than current solar trackers. Moreover, due to the incorporation of a camera, the new system allows to document residual pointing errors and to point onto the solar disc centre even in case of variable intensity distributions across the source due to cirrus or haze.

1 Introduction

Ground-based solar absorption FTIR measurements are performed at numerous sites worldwide to monitor trace gases in the terrestrial atmosphere. Prominent FTIR networks are the "Network for the Detection of Atmospheric Composition Change" (NDACC, http://www.ndsc.ncep.noaa.gov), operating in the mid infrared spectral region (MIR) and encompassing over 20 measurement sites worldwide and the "Total Carbon Column Observing Network" (TCCON, www.tccon.caltech.edu), focusing mainly on CO_2 measurements in the near infrared (NIR) at about 20 sites worldwide (Toon et al., 2009). As one aims to increase the accuracy of the retrieved column-averaged abundances of atmospheric constituents continuously, new challenges arise.

In the past, major efforts were undertaken to improve the spectrometer itself, such as the ILS-characterization (Hase, Blumenstock, and Paton-Walsh, 1999), applying a DC-correction on the interferogram (Keppel-Aleks et al., 2007), improving the sampling accuracy (Messerschmidt et al., 2010) and characterization of detector non-linearities (Abrams, Toon and Schindler, 1994). But in order to reach the requested accuracy, the

AMTD
3, 4865–4887, 2010

tracking quality also has to be considered, which is still an open issue. The current approach to reach an optimal tracking precision is to use a quadrant-diode to register deviations from the precalculated pointing direction of the tracking system. The diode signal is then fed in the control loop of the tracker (Adrian et al., 1994), (Notholt and Schrems, 1995) and (Washenfelder et al., 2006). However, these systems do not achieve the required accuracy in some conditions, especially at low solar elevation. In addition they are prone to misalignments between the line-of-sight (LOS) defined by the quadrant sensor and the LOS of the spectrometer which cause systematic and non-recoverable errors. They also require strict conditions on the shape and intensity distribution of the light source. We overcame these problems by controlling the tracking with a new camera-based system.

2 Importance of the tracking accuracy

When using the sun as a light source for atmospheric absorption spectroscopy, one usually aims to point the interferometer's field-of-view on the centre of the solar disc. This is equivalent to centre the solar disc on the circular entrance field stop of the interferometer. Any deviations from the assumed LOS introduces errors in the retrieval of the gas-concentrations of the atmosphere. The main problem caused by a pointing error is that the actual observed air mass differs from the air mass assumed in the analysis. The error resulting from a line-of-sight error depends strongly on the zenith angle of the sun and is shown in Fig. 1. With a desired tracking range down to 80° solar zenith angle (SZA), one gets about 10% air mass change per degree SZA-change. TCCON currently strives for a total CO_2 column precision of 0.1% in order to constrain the interhemispheric gradient (Olsen and Randerson, 2004). To achieve this overall precision, an error due to the tracking of smaller than 0.05% is desirable. If one wants to maintain this for a tropospheric gas up to a solar zenith angle of 80°, a tracking accuracy of about 19 arc s is required.

AMTD
3, 4865–4887, 2010

Although it is possible to reduce the tracker impact by rationing the CO_2 slant column over the O_2 slant column (which can be estimated from the ground pressure and the H_2O slant column), an excellent tracking knowledge is nevertheless highly desirable, because this allows to recognize other problems by monitoring the observed O_2 column. Moreover, in the MIR spectral region, no reference of similar precision is available, so the calibration using O_2 is not feasible in case of NDACC measurements.

3 Tracking accuracy with current quadrant-diode setups

An additional effect of mispointing of the solar tracker is to generate a Doppler shift of the solar lines with respect to the telluric spectral features due to the solar rotation. The synodic rotation period of the sun is about 26.75 days, which corresponds to an observed equatorial solar velocity of about 1890 $\frac{m}{s}$ (Lang, 1991). A mispointing along the solar equator of 1 arc min translates into a Doppler scaling $\frac{\Delta\nu}{\nu}$ of 3.9×10^{-7}. If this effect is considered in the analysis by fitting a separate shift for the solar background lines, the effects on the trace gas analysis are minor, but it gives a useful method to estimate the pointing quality at hand. Note, however, that the mispointing cannot be retrieved from the observed Doppler shifts, because there is no sensitivity along the direction parallel to the solar rotation axis.

In Fig. 2, solar shift analysis results from our measuring site in Kiruna are shown, indicating an accuracy of $\sqrt{2} \times \pm 69'' \approx \pm 98$ arc s, probably a typical value for current tracker setups. At the TCCON measurement site in Izaña, we reach an accuracy of $\pm$ 50 arc s for the time after May 2007 with a quadrant diode setup. These accuracies are not sufficient for the desired gas-retrieval precision of 0.1%, as they result in an air mass change of about 0.3% and 0.14% at a solar zenith angle of 80°, respectively. For these analysis we used the software PROFFIT Ver. 9.6 which was developed at IMK (Hase et al., 2004). A model of the solar absorption lines is included in this code (Hase et al., 2006) and (Hase, Wallace, McLeod, Harrison and Bernath, 2010). The solar line

AMTD
3, 4865–4887, 2010

list for the NIR-region was provided by G. Toon, JPL (G. Toon, personal communication, 2004).

4 Camtracker setup

The demonstration setup is located at our measurement site near Karlsruhe, Germany (49.10° N, 8.44° E). We use a 20 ft container to house our IFS 125HR FTIR-spectrometer from Bruker Optics GmbH, with an OPD_{max} of 257 cm. This is equipped with a CaF_2 beamsplitter, an InSb and an InGaAs-detector. The tracker is mounted on top of the container, and has, except for the motor-types, the same technical setup as our trackers in Izaña and Kiruna, which are operational since 1999 and 1998, respectively. The mechanical setup of the altazimuthal tracker is shown in Fig. 3. The sunlight is reflected into the container by two plane ellipse shaped mirrors, having 12 cm as the projected diameter. The first mirror is built on a Newport RV80PP rotation stage, so that different elevation angles can be accessed. The whole setup with both mirrors is mounted on a Newport RV160PP rotation stage, so that desired azimuthal directions can be reached. This motor is able to move a considerable weight and is also carrying the "letter-box" shaped cover of the tracker so that the opening is always orientated into the observing direction. This cover can be opened, closed and sealed with pressurized air and was developed by the IMK in cooperation with Impres GmbH (http://www.impres.de). The RV160PP offers a hollow axle diameter of 11 cm, through which the light falls vertically downwards into the container. The two motors are connected to a Newport XPS-Controller unit inside the container.

The optical setup inside the container is shown in Fig. 4. The optical path from the second tracking mirror to the input window of the spectrometer spans about 2.5 m. The radiation is focused onto the input field stop of the spectrometer by an off-axis parabolic mirror. The field stop is realized by a flat metal wheel with round holes of different diameters, which can be rotated to select a desired field stop diameter. It is tilted a few degrees with respect to the light passing it to prevent reflections inside

AMTD
3, 4865–4887, 2010

the spectrometer. The input field stop diameters used are smaller than the size of the picture of the solar disc on the field stop wheel of about 3.8 mm, resulting from the focal length of the parabolic mirror (418 mm). After passing the field stop, the light is parallelized by a collimator and then enters the interferometer and finally is focused onto the detectors.

To monitor and control the pointing of our tracker, we use a standard CMOS USB-camera (VRmagic VRM C-9+PRO BW with 1280 × 1024 pixels) as an optical feedback, which records the input side of the field stop wheel. The camera is equipped with a standard objective and appropriate optical filters to adjust for the illumination level. Due to the wavelength dependent refractivity of air, it is in case of NIR and MIR spectroscopic observations advantageous to equip the camera with an infrared longpass filter which transmits radiation beyond 750 nm. In connection with the spectral sensitivity of current CCD and CMOS-cameras this choice defines a bandpass of about 100 nm width. (For further details on atmospheric dispersion see Sect. 7.) The solar disc has a diameter of about 240 pixels on the recorded pictures, the field stop diameters cover a range from about 20 to 160 pixels. The pictures are evaluated on a standard PC in real-time by our newly developed program using appropriate image processing algorithms, to determine the actual tracking accuracy and to calculate required corrections to the astronomical tracking mirror angles. The program then sends the tracking-commands to the motor-controller (Newport XPS) via an IP-connection.

5 Principle of operation

The operation principle of our tracker in Karlsruhe is based on a combination of astronomical algorithms to provide the coarse mirror angles with a superposition of small corrections to these angles derived from the optical feedback provided by the camera. The recorded pictures are evaluated by our software “CamTrack” in real-time, in order to determine both the central position of the field stop opening and the solar disc. Then the necessary mirror angle corrections to “move” the solar disc on the field stop wheel

AMTD
3, 4865–4887, 2010

to the desired position relative to the input field stop opening are calculated and sent to the tracking system. These steps are continuously performed about three times per second. If no usable positions for the solar disc and the field stop opening can be determined, for example due to clouds, the system continues tracking on the basis of the astronomical coordinates together with previously saved offset values for similar tracking angles.

The main steps in determining the central positions from the camera pictures are the following:

1. Finding an appropriate threshold value to separate the bright area illuminated by the sun from the dark, non-illuminated rest of the field stop wheel, and the dark opening of the field stop.

2. Creating a binary picture by applying the threshold, and finding the contours along the obtained areas.

3. Fitting ellipses along the contours (in a least squares sense).

4. Performing consistency checks, if the obtained ellipses can be the contours of the solar disc and the field stop opening in terms of criteria like radius, position and eccentricity.

5. If the previous step was successful, taking the centres of the ellipses as centres of the solar disc and the round field stop opening.

Figure 5 shows a subframe of 2 typical pictures of the camera. In cases where the field stop opening is not inside the solar disc, it is, in general, not visible. Then the solar disc is moved along a search pattern over the field stop wheel until the opening is found.

In order to calculate the corrections to the tracker mirror angles, one needs the information on how the mirrors have to move, to realign the solar disc on the field stop. However, this correlation is not constant, but depends on the solar position on the sky. One way to get it, is to model the whole mirror-system including the camera,

AMTD
3, 4865–4887, 2010

which, however, is a quite complex task. A simple approach is to sequentially move the mirror angles a few small defined steps, and to register the resulting shift (direction and distance) of the solar disc in terms of camera-pixels. This procedure can't be performed during a FTIR-measurement. Therefore we use a combination of the two procedures, which includes a simplified simulation of our two tracking mirrors only, and an experimentally determined correlation, at the beginning of the tracking, to initialize the simulation. This has the advantage, that the effects of all the optical elements after the first two tracking mirrors are determined experimentally. For example, if the camera position or orientation changes or some additional mirrors are used, the only thing to do is to reperform the initialization sequence to adapt the simulation.

6 Advantages of the camera setup

The main reasons to choose the camera set-up instead of a quadrant-diode, which is the current solution applied in the NDACC and the TCCON, is that it results in a very exact tracking, it is easy to setup and very robust:

– Using the camera-information, one can determine both the position of the centre of the solar disc on the field stop wheel and the opening of the stop at the same time. Since the input stop itself defines the measurement-direction of the spectrometer one has direct information about the pointing and its errors. In other words, the camera-based optical feedback system is self-calibrating. Systematic shifts are avoided, as they can easily occur with a quadrant-diode setup. Displacements of the camera into any direction do not matter as long as the camera records a sufficiently focused picture of the solar disc and the field stop opening. This, as the only prerequisite, makes the system very easy to set-up and robust. Combined with an excellent spacial resolution of current cameras, this leads to a very precise tracking of the sun, as it is shown in Sect. 7.

AMTD
3, 4865–4887, 2010

- A very important advantage over a quadrant-diode-setup is the ability to precisely track light sources which have a variable intensity over their surface. For the sun, this can be caused by a rather thin cloud layer or mist which dims a part of the sun, as it often happens at low solar angles. As long as one still can determine the rim of the solar disc, it is possible to determine the centre of the disc and to maintain the precise LOS steering. An example can be seen in Fig. 5. A quadrant-diode, however, detects the centre of intensity instead, which then is centred onto the input field stop.

- Resulting from the fact that the rim of the light source can be used instead of the centre of intensity, the system provides the ability to track non-round light sources, as the partially illuminated moon.

- By storing the pictures, even in the occurrence of tracking problems, one can determine the actually existing pointing directions later on and use them when evaluating the FTIR spectra. The stored pictures also offer a way to reveal the causes of unexpected intensity variations during subsequent inspections of the interferograms (e.g. moving objects as clouds, birds, airplanes or transit of sun across fixed obstacles, e.g. contour of antennas, buildings, trees).

- The camera control loop is very easy to set up since no other optical elements except for the camera are needed. Its only prerequisite is the existence of an field stop which scatters some radiation back, so it is widely applicable.

7 Tracking accuracies and results

A first approach to determine the tracking accuracy of the CamTracker is to look at the distance of the centres of the two ellipses, which correspond to the solar disc and the field stop opening. This may not exactly be the actual accuracy of the pointing, since there may be deviations between the ellipse and the actual rim of the solar disc and

AMTD
3, 4865–4887, 2010

residual errors resulting from small perspective distortions. Still we expect a useful quantification of the pointing error due to the motor resolution and mechanical backlash. Knowing the recorded solar disc diameter in camera-pixels and its angular size on the sky of about 32 arc min, one can transform the ellipse-centre distances in pixels to tracking-angle deviations in degrees. Figure 6 shows a plot of these deviations over a time period of more than 8 h, from which a tracking accuracy of 3.7 arc s and a very small systematic error of about 0.3 arc s can be derived.

We also evaluated the solar Doppler line shifts for the spectra measured in Karlsruhe with the new camera setup in the NIR spectral domain, as described in Sect. 3. An example is shown in Fig. 7 which illustrates the effect of a tracking offset of 5 arc min.

The solar shifts which were determined by this kind of analysis, are shown in Figs. 8 and 9. Assuming the tracking offsets to be of equal size along the direction perpendicular to the solar equator, the estimated tracking accuracy has a precision of about ± 11 arc s ($1\,\sigma$). The precision of the Doppler analysis has been crosschecked using a second microwindow (from 6248.3 to 6249.9 wavenumbers) and is about $2.5''$. An additional source of uncertainty in the analysis is the Doppler shift of the terrestrial reference lines due to wind, typically below $5''$ (assuming wind speeds below $10\,\frac{\mathrm{m}}{\mathrm{s}}$). The outstanding tracker precision is significantly better than the projected $19''$ and therefore sufficient to measure gas column concentrations with a precision below 0.1% for solar zenith angles smaller than 80°.

Before the 22 September 2010, an older version of CamTrack was operating, showing an ellipse deviation of 6.5 arc s (compare Fig. 6). Therefore we expect the tracking accuracy to be even better than 11 arc s for current and future measurements. In the presented time series, the position and orientation of the camera changed fequently, due to modifications of our components in front of the FTIR-spectrometer. This shows the robust mode of operation of the system and its independence from the position of the camera.

AMTD
3, 4865–4887, 2010

8 Implications for data analysis

In order to take full advantage of the unprecedented precision which is achievable with the new CamTracker, we give a short discussion on implications for the data analysis in this section.

Firstly, it should be taken into account that the NIR/MIR ray path relevant for the quantitative analysis of the spectrum is not identical with the VIS/NIR ray path defined by the camera. Due to atmospheric refraction, the ray path is bent, its curvature being a function of pressure, H_2O volume mixing ratio (VMR) and wavelength (Hase and Höpfner, 1999; Peck and Reeder, 1972; Jones, 1981; Matsumoto, 1982; Ciddor, 1996). Since the camera pointing refers to the centre of the VIS/NIR solar disc, the apparent angle of this LOS has to be used in the analysis of the spectrum (the actual LOS of the IR bandpass which is analyzed is not ideally centred on the field stop). Therefore, in the quantitative analysis of the spectrum, the raytracing must reproduce the apparent solar elevation defined by the VIS/NIR camera bandpass at the observer, but use the refractive index appropriate for the IR bandpass of the spectrometer. Quantitatively, at 80° SZA, the total deviation of the beam due to refraction is on the order of 300 arc s, a 750 nm ray being deviated by an additional 3 arc s compared to a 2 µm ray.

The second aspect is the temporal extent of the FTIR measurement. Depending on the spectral resolution applied, the recording of an interferogram requires up to several minutes. Current analysis schemes for ground-based FTIR-spectra assume a single pencil-beam LOS, whereas the measurement covers a finite range of elevation angles. A detailed discussion of this problem is beyond the scope of this technical paper, which deals with the CamTracker setup and precision verification. The optimum choice of an effective solar elevation angle and the allowable measurement duration as function of latitude and solar elevation will be addressed in a subsequent paper dealing with the impact of the variable solar elevation from the viewpoint of the analysis.

AMTD
3, 4865–4887, 2010

9 Conclusions

The presented camera set-up in combination with the real-time image evaluation and tracking software "CamTrack" was shown to result in an outstanding tracking accuracy of better than 11 arc s. This quality level was maintained over a period of 5 months, despite frequent changes of the camera position, showing the robustness of the operation principle. The system is very easy to setup and applicable in many situations, where there is the need of positioning the radiation of a light source on the field stop of a spectrometer.

Acknowledgements. We would like to thank the NASA Goddard Space Flight Center for providing NCEP daily temperature and pressure profiles (via the automailer system) which were used for the Doppler analysis and for the calculation of the solar refraction.

References

Abrams, M. C., Toon, G. C., and Schindler, R. A.: Practical example of the correction of Fourier-transform spectra for detector nonlinearity, Appl. Optics, 33(27), 6307–6314, doi:10.1364/AO.33.006307, 1994. 4866

Adrian, G. P., Baumann, M., Blumenstock, T., Fischer, H., Friedle, A., Gerhardt, L., Maucher, G., Oelhaf, H., Scheuerpflug, W., Thomas, P., Trieschmann, O., and Wegner, A.: First results of ground-based FTIR measurements of atmospheric trace gases in North Sweden and Greenland during EASOE, Geophys. Res. Lett., 21, 1343, 1994. 4867

Ciddor, P. E.: Refractive index of air: new equations for the visible and near infrared, Appl. Optics, 35, 1566–1573, 1996. 4875

Hase, F., Blumenstock, T., and Paton-Walsh, C.: Analysis of the instrumental line shape of high-resolution Fourier transform IR spectrometers with gas cell measurements and new retrieval software, Appl. Optics, 38, 3417–3422, 1999. 4866

Hase, F. and Höpfner, M.: Atmospheric raypath modelling for radiative transfer algorithms, Appl. Optics, 38, 3129–3133, 1999. 4875

Hase, F.: Inversion von Spurengasprofilen aus hochaufgelösten bodengebundenen FTIR-Messungen in Absorption, Dissertation, FZK Report No. 6512, http://www-imk.fzk.de/asf/ftir/disshase.pdf, last access: 28 October 2010, Forschungszentrum Karlsruhe, Germany, 2000. 4879

Hase, F., Hannigan, J. W., Coffey, M. T., Goldman, A., Höpfner, M., Jones, N. B., Rinsland, C. P., and Wood, S. W.: Intercomparison of retrieval codes used for the analysis of high-resolution, ground-based FTIR measurements, J. Quant. Spectrosc. Ra., 87, 25-52, 2004. 4868

Hase, F., Demoulin, P., Sauval, A. J., Toon, G. C., Bernath, P. F., Goldman, A., Hannigan, J. W., and Rinsland, C. P.: An empirical line-by-line model for the infrared solar transmittance spectrum from 700 to 5000 cm^{-1}, J. Quant. Spectrosc. Ra., 102, 450–463, doi:10.1016/j.jqsrt.2006.02.026, 2006. 4868

Hase, F., Wallace, L., McLeod, S. D., Harrison, J. J., and Bernath, P. F.: The ACE-FTS atlas of the infrared solar spectrum, J. Quant. Spectrosc. Ra., 111(4), 521–528, 2010. 4868

Huster, S.: Bau eines automatischen Sonnenverfolgers fr bodengebundene IR-Absorptionsmessungen, Diploma Thesis, Forschungszentrum Karlruhe, Universität Karlsruhe, 1998. 4881

Jones, F. E.: The refractivity of air, J. Res. Nat. Bur. Stand., 86, 27-32, 1981. 4875

Keppel-Aleks, G., Toon, G. C., Wennberg, P. O., and Deutscher, N. M.: Reducing the Impact of Source Brightness Fluctuations on spectra obtained by FTS, Appl. Optics, 46, 4774-4779, 2007. 4866

Lang, K. R.: Astrophysical Data: Planets and Stars, Springer Verlag, ISBN 0-387-97109-2, 1991. 4868

Matsumoto, H.: The Refractive Index of Moist Air in the 3-µm Region, Metrologia, 18, 49–52, doi:10.1088/0026-1394/18/2/001, 1982. 4875

Messerschmidt, J., Macatangay, R., Notholt, J., Petri, C., Warneke, T., and Weinzierl, C.: Side by side measurements of CO_2 by ground-based Fourier transform spectrometry (FTS), Tellus B, 62, 749-758, 2010. 4866

Miller, C. E., Crisp, D., DeCola, P. L., Olsen, S. C., Randerson, J. T., Michalak, A. M., Alkhaled, A., Rayner, P., Jacob, D. J., Suntharalingam, P., Jones, D. B. A., Denning, A. S., Nicholls, M. E., Doney, S. C., Pawson, S., Boesch, H., Connor, B. J., Fung, I. Y., O'Brien, D., Salawitch, R. J., Sander, S. P., Sen, B., Tans, P., Toon, G. C., Wennberg, P. O., Wofsy, S. C., Yung, Y. L., and Law, R. M.: Precision requirements for space-based XCO_2 data, J. Geophys. Res., 112, D10314, doi:10.1029/2006JD007659, 2007.

Discussion Paper | Discussion Paper | Discussion Paper | Discussion Paper |

Notholt, J., Beninga, I., and Schrems, O.: Ground-based FTIR spectroscopic absorption measurements of stratospheric trace gases in the Arctic with the sun and the moon as light sources, J. Mol. Struct., 347, 407–416, 1995.

Notholt, J. and Schrems, O.: Shipborne FT-IR Measurements of Atmospheric Trace Gases on a South (33° S) to North (53° N) Atlantic Traverse, Appl. Spectrosc., 49, 10, 1525–1527, 1995. 4867

Olsen, S. C. and Randerson, J. T.:, Differences between surface and column atmospheric CO_2 and implications for carbon cycle research, J. Geophys. Res., 109, D02301, doi:10.1029/2003JD003968, 2004. 4867

Peck, E. R. and Reeder, K.: Dispersion of air, J. Opt. Soc. Am., 62(8), 958–962, doi:10.1364/JOSA.62.000958, 1972. 4875

Toon, G., Blavier, J.-F., Washenfelder, R., Wunch, D., Keppel-Aleks, G., Wennberg, P., Connor, B., Sherlock, V., Griffith, D., Deutscher, N., and Notholt, J.: Total Column Carbon Observing Network (TCCON), http://www.tccon.caltech.edu/publications/OSA_FTS_Meeting_20090323.pdf, last access: 28 October 2010, 2009. 4866

Washenfelder, R. A., Toon, G. C., Blavier, J.-F., Yang, Z., Allen, N. T., Wennberg, P. O., Vay, S. A., Matross, D. M., and Daube, B. C.: Carbon dioxide column abundances at the Wisconsin Tall Tower site, J. Geophys. Res., 111, D22305, doi:10.1029/2006JD007154, 2006. 4867

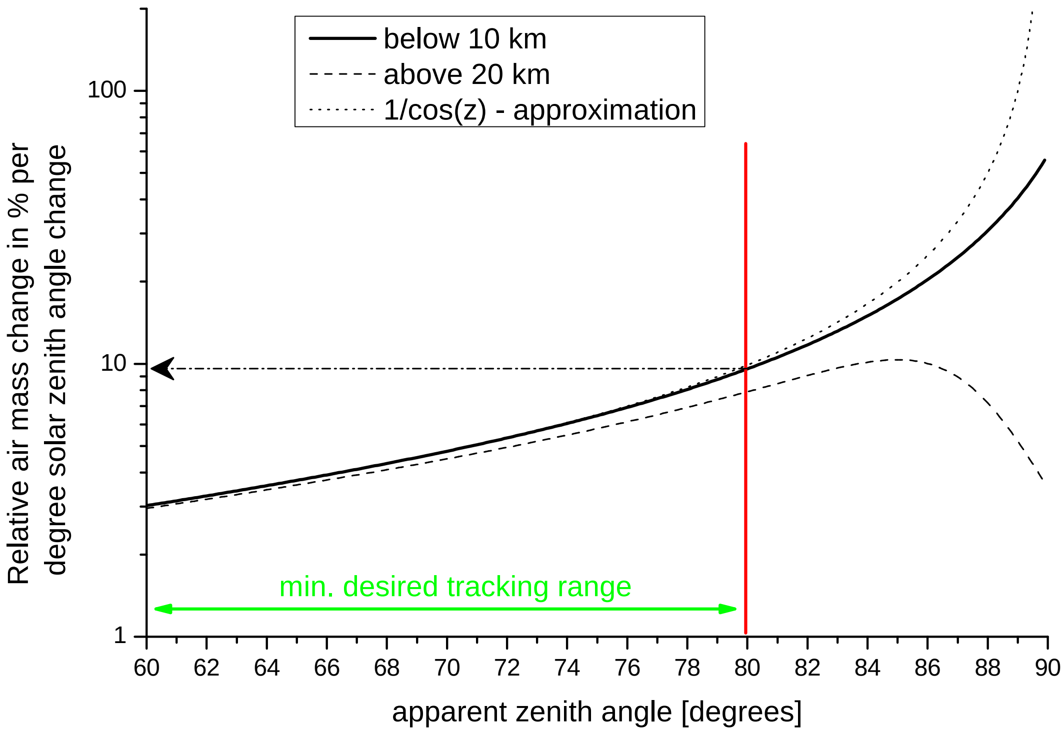

Fig. 1. Sensitivity of the effective air mass as function of solar zenith angle for the observation of a tropospheric gas with constant VMR up to 10 km (bold line), for the observation of a stratospheric gas with constant VMR above 20 km (dashed) and for the often used analytical approximation 1/cos(z) (dotted). (Graph taken from Hase, 2000.)

AMTD
3, 4865–4887, 2010

Camera controlled high precise solar tracker

M. Gisi et al.

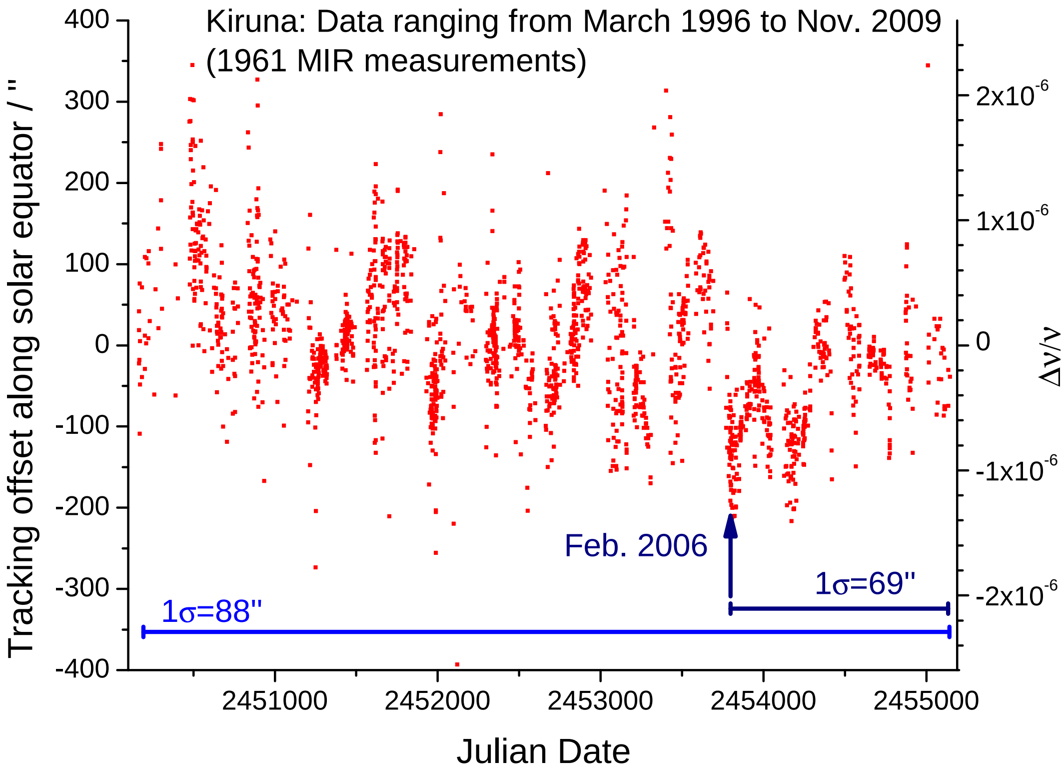

Fig. 2. Tracking angle offset determined by solar shifts for the measurement site in Kiruna as a typical NDACC-station. For both directions, a tracking accuracy of ± 98 arc s (1 σ) can be estimated for the time after February 2006. The evaluated spectral window ranged from 2703.2 to 2705.3 wavenumbers.

AMTD
3, 4865–4887, 2010

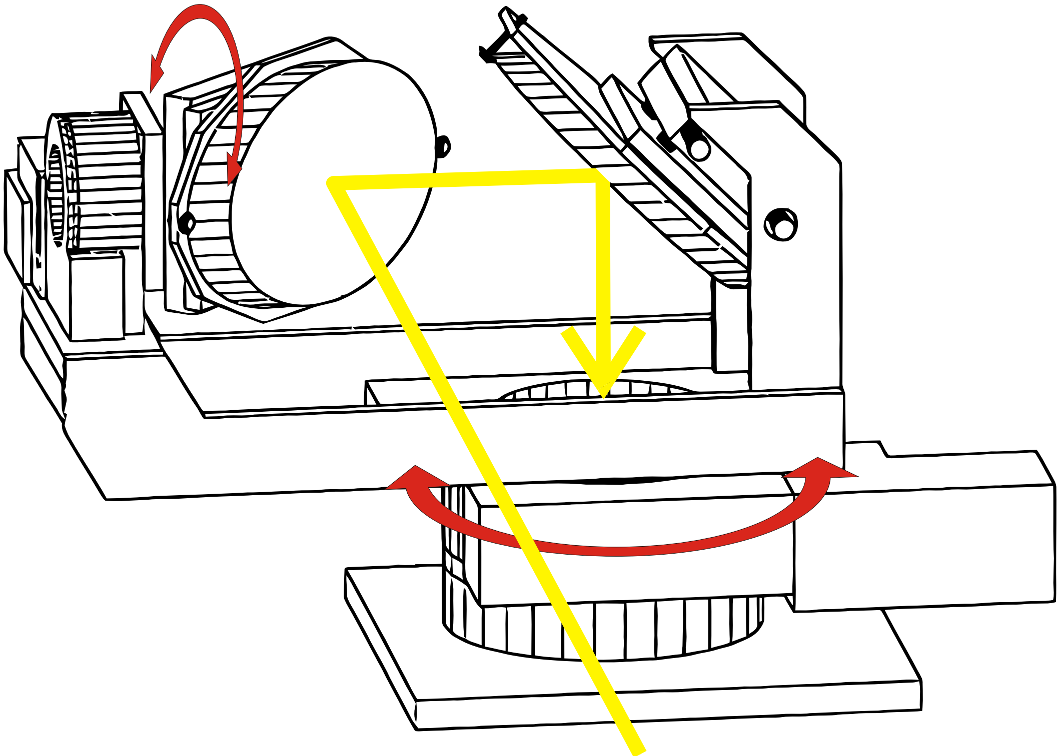

Fig. 3. Schematic drawing of the tracker used. (Picture taken from Huster, 1998.)

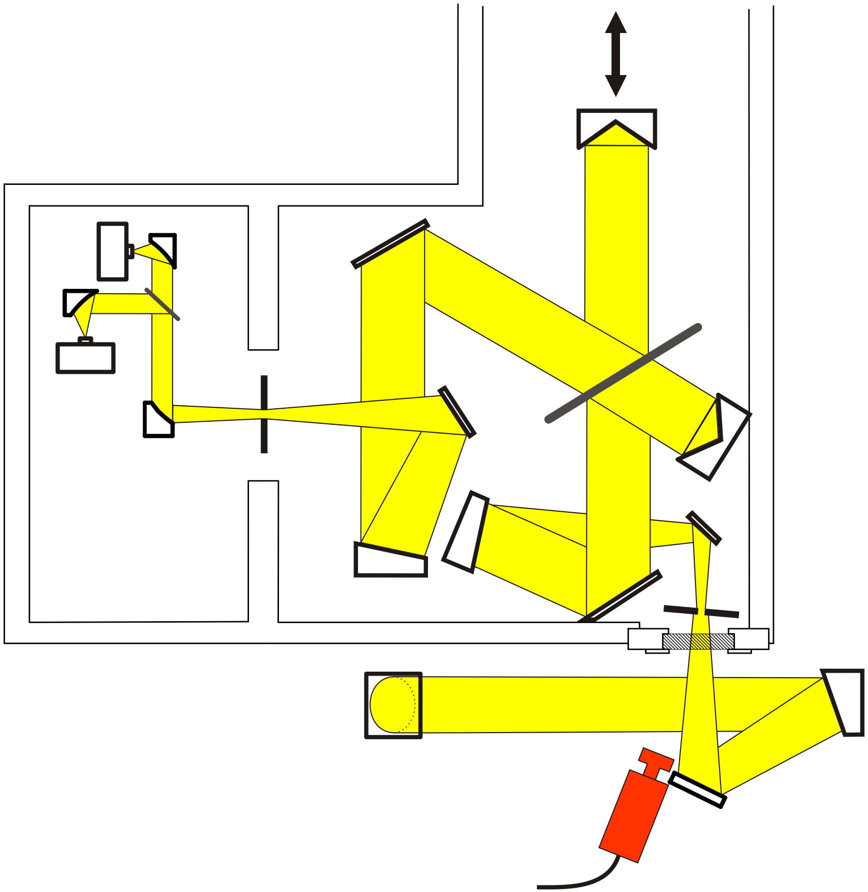

Fig. 4. Schematic drawing of the top-view of the camera set-up and the light path in front of and inside the spectrometer. The light falls from the tracker on the roof, perpendicular to the plane of the drawing onto the first mirror. The camera records the illuminated input field stop wheel.

AMTD

3, 4865–4887, 2010

Camera controlled high precise solar tracker

M. Gisi et al.

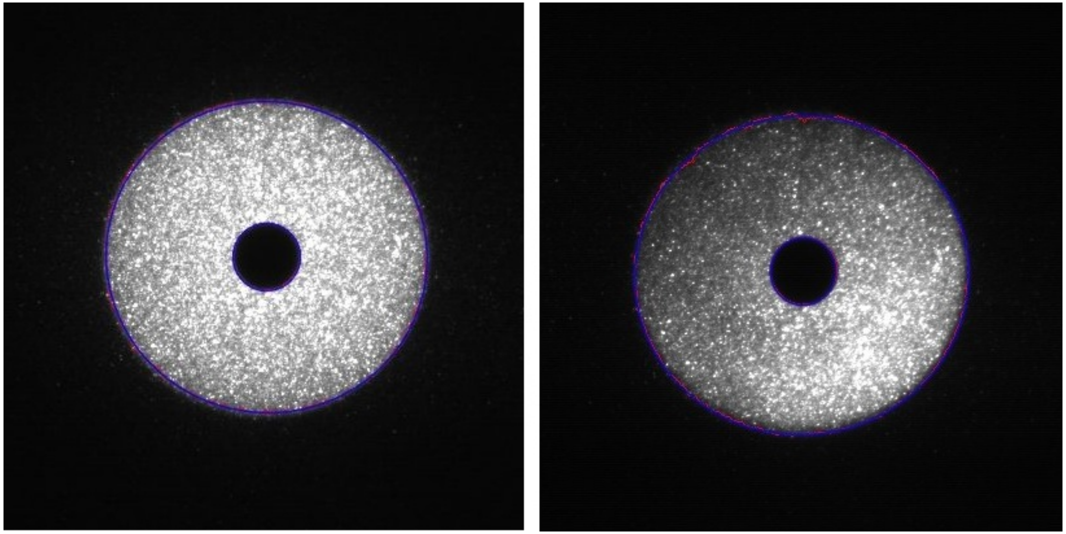

Fig. 5. Two pictures of the camera. The ellipses, which have been retrieved by the image processing algorithms are painted in blue on top of the original image. The solar disc and the field stop opening have diameters of 244 and 52 pixels respectively. The field stop diameter used was 0.8 mm. The right picture shows a correct positioning of the solar disc relative to the field stop opening despite strong intensity variations resulting from clouds, which would be impossible using a quadrant diode.

AMTD
3, 4865–4887, 2010

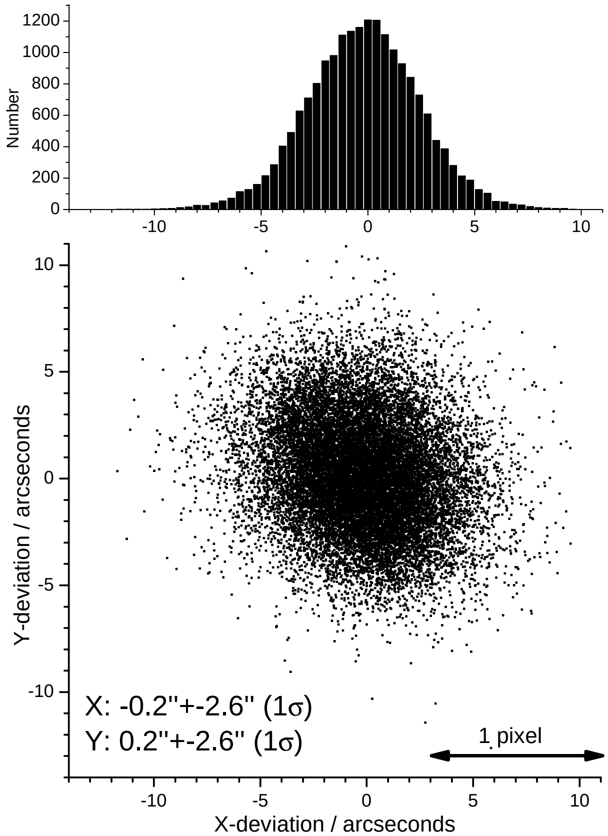

Fig. 6. Distance between the centres of the 2 fitted ellipses corresponding to the solar disc and the field stop opening. The units are given in tracking angle deviations. The data has a 2-D 1 σ interval of less than 4 arc s and was recorded at 22 September 2010, 10:29–16:43 UTC and 23 September 2010, 07:54–12:36 UTC, in two seconds intervals with a new version of CamTrack. The previous version, used before the 22 September 2010, had 2-D 1 σ interval of 6.5 arc s.

AMTD
3, 4865–4887, 2010

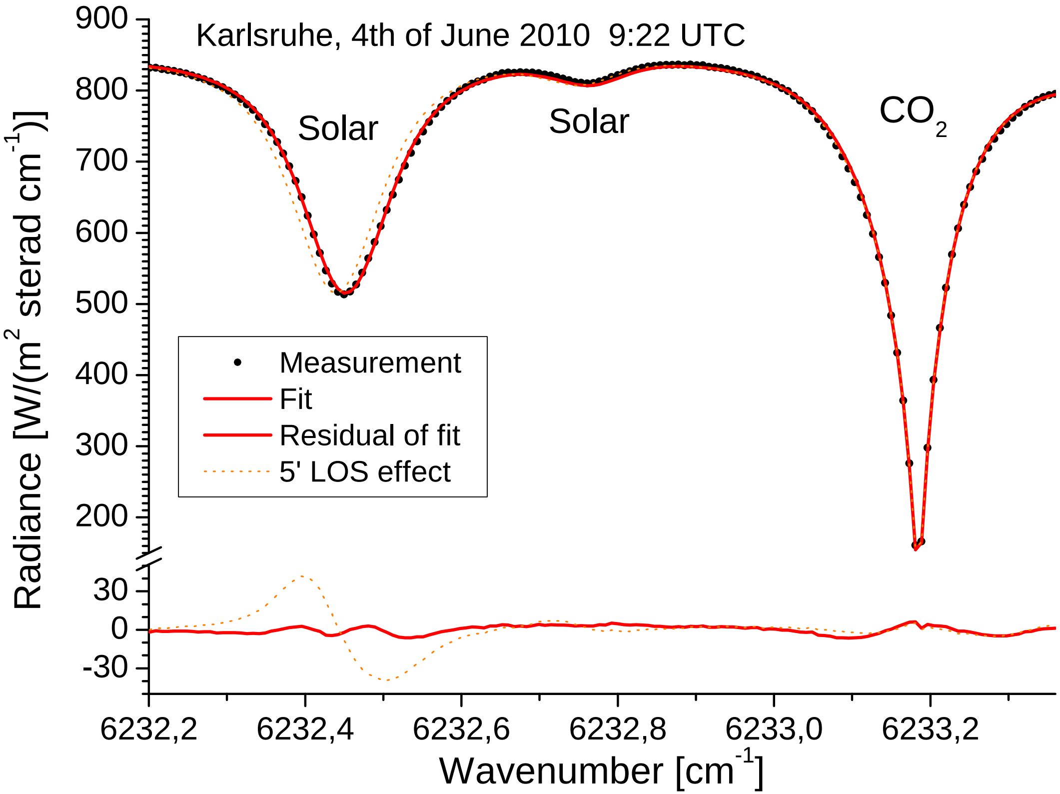

Fig. 7. Spectral microwindow to determine the solar shift for the spectra recorded in Karlsruhe. The black points correspond to the actual measurement, the red continuous lines to the fit and the residual. The dashed lines correspond to a simulation and for a pointing offset of 5 arc min along the solar equator.

AMTD
3, 4865–4887, 2010

Camera controlled high precise solar tracker

M. Gisi et al.

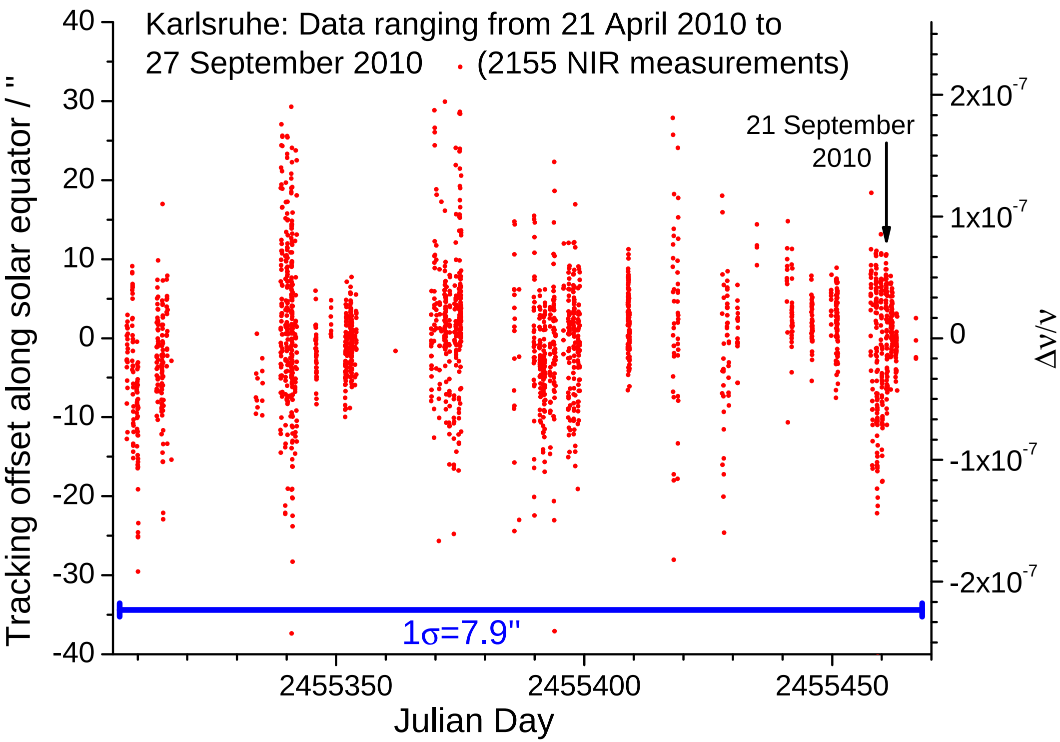

Fig. 8. Tracking angle offset along the solar equator determined by solar line shifts for 56 measurement days of observation at the Karlsruhe site. For both directions (2-D) a tracking accuracy of smaller than $\sqrt{2} \times \pm 7.9 = \pm 11.2$ arc s ($1\,\sigma$) can be estimated. The evaluated spectral window ranged from 6232.2 to 6233.36 wavenumbers (see Fig. 7).

AMTD
3, 4865–4887, 2010

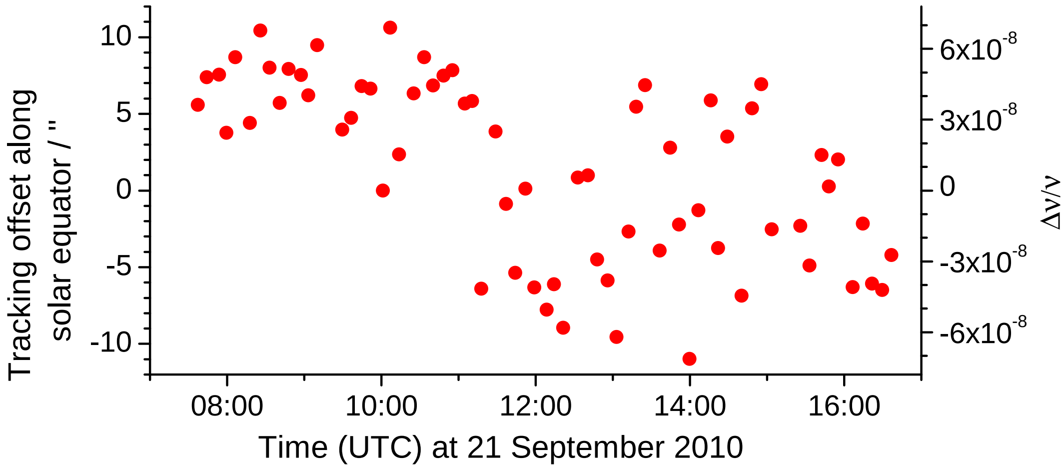

Fig. 9. Enlarged part of Fig. 8 for one exemplary day of measurement (21 September 2010).

AMTD
3, 4865–4887, 2010